

Mechanical and wear behaviour of hot-pressed 304 stainless steel matrix composites containing TiB₂ particles

Sahoo, S.; Jha, B.B.; Mahata, T.; Sharma, J.; Murthy, T.S.R.C.; Mandal, A.

DOI:

[10.1007/s12666-019-01588-1](https://doi.org/10.1007/s12666-019-01588-1)

License:

None: All rights reserved

Document Version

Peer reviewed version

Citation for published version (Harvard):

Sahoo, S, Jha, BB, Mahata, T, Sharma, J, Murthy, TSRC & Mandal, A 2019, 'Mechanical and wear behaviour of hot-pressed 304 stainless steel matrix composites containing TiB₂ particles', *Transactions of the Indian Institute of Metals*, vol. 72, no. 5, pp. 1153–1165. <https://doi.org/10.1007/s12666-019-01588-1>

[Link to publication on Research at Birmingham portal](#)

Publisher Rights Statement:

Checked for eligibility: 17/09/2019

This is a post-peer-review, pre-copyedit version of an article published in *Transactions of the Indian Institute of Metals*. The final authenticated version is available online at: <http://dx.doi.org/10.1007/s12666-019-01588-1>

General rights

Unless a licence is specified above, all rights (including copyright and moral rights) in this document are retained by the authors and/or the copyright holders. The express permission of the copyright holder must be obtained for any use of this material other than for purposes permitted by law.

- Users may freely distribute the URL that is used to identify this publication.
- Users may download and/or print one copy of the publication from the University of Birmingham research portal for the purpose of private study or non-commercial research.
- User may use extracts from the document in line with the concept of 'fair dealing' under the Copyright, Designs and Patents Act 1988 (?)
- Users may not further distribute the material nor use it for the purposes of commercial gain.

Where a licence is displayed above, please note the terms and conditions of the licence govern your use of this document.

When citing, please reference the published version.

Take down policy

While the University of Birmingham exercises care and attention in making items available there are rare occasions when an item has been uploaded in error or has been deemed to be commercially or otherwise sensitive.

If you believe that this is the case for this document, please contact UBIRA@lists.bham.ac.uk providing details and we will remove access to the work immediately and investigate.



Mechanical and wear behavior of hot pressed 304 stainless steel matrix composites containing TiB₂ particles

Journal:	<i>Particulate Science and Technology</i>
Manuscript ID	UPST-2018-1788
Manuscript Type:	Original Article
Date Submitted by the Author:	31-Jul-2018
Complete List of Authors:	Sahoo, Silani; Institute of Minerals and Materials Technology CSIR, Advanced Materials Technology Department Jha, Bharat; CSIR-Central Glass & Ceramic Research Institute, Business Development & Standardisation Division Mahata, Tarasankar; Bhabha Atomic Research Centre, Powder Metallurgy Division Sharma, Jyothi; Bhabha Atomic Research Centre, Powder Metallurgy Division Murthy, Tammana; Bhabha Atomic Research Centre, Materials Processing and Corrosion Engineering Division Mandal, Animesh; Indian Institute of Technology Bhubaneswar - Toshali Campus, School of Minerals, Metallurgical and Materials Engineering
Keywords:	304 stainless steel, TiB ₂ , hot pressing, microstructure, mechanical properties < ceramics, wear

SCHOLARONE™
Manuscripts

Mechanical and wear behavior of hot pressed 304 stainless steel matrix composites containing TiB₂ particles

Silani Sahoo^{1*}, Bharat B Jha², Tarasankar Mahata³, Jyothi Sharma³, Tammana SRCh Murthy⁴ and Animesh Mandal⁵

¹ Advanced Materials Technology Department, CSIR-Institute of Minerals and Materials Technology, Bhubaneswar, 751013, Odisha, India

² Business Development & Standardisation Division, CSIR-Central Glass & Ceramic Research Institute, Kolkata, 700032, West Bengal, India

³ Powder Metallurgy Division, Bhabha Atomic Research Centre, Navi Mumbai – 400703 Maharashtra, India

⁴ Materials Processing and Corrosion Engineering Division, Bhabha Atomic Research Centre, Mumbai - 400 085, Maharashtra, India

⁵ School of Minerals, Metallurgical and Materials Engineering, Indian Institute of Technology Bhubaneswar, Bhubaneswar, 751007, Odisha, India

Abstract

In the present article, mechanical and wear behavior of hot pressed 304 stainless steel matrix composites containing 2 and 4 vol.% TiB₂ particles were investigated. A density of over 92% was achieved at optimum hot pressing temperature and volume fraction of TiB₂ particles. Microhardness and yield strength of the composites was found to be improved remarkably as compared to their unreinforced counterpart. The enhancement of mechanical properties of the composites was discussed in light of their microstructural aspects and different possible strengthening mechanism models. Taylor strengthening was found to be dominant strengthening mechanism as compared to Orowan strengthening and load bearing effect. Dry sliding wear behavior was also investigated under load of 35 N at sliding speed 0.3 m/s. The wear resistance of the composites were found to be improved owing to uniform distribution of hard TiB₂ particles. Based on our findings, it was concluded that processing parameters and amount of TiB₂ have significant influence on mechanical and wear behavior of steel matrix composites.

Keywords: 304 stainless steel; TiB₂; hot pressing; microstructure; mechanical properties; wear

***Corresponding author:** Email: silanisahoo@immt.res.in

1. Introduction

Metal matrix composites (MMCs) are tailored to possess properties not exhibited either by matrix or the reinforcement. The metallic matrix may be aluminium, copper, magnesium, titanium, zinc and their alloys (Akhtar 2014; Rana and Liu 2014; Springer et al. 2015). Improvement in the properties of MMCs such as hardness, wear and corrosion resistance, specific modulus, ductility and fracture toughness represents a major challenge due to its dependence on interplay of several processing and microstructural parameters. These microstructural parameters are influenced by volume fraction of ceramic reinforcements, shape and size of reinforcements, interface between ceramic reinforcement and matrix material, composition of matrix, defects, cracks and distribution of reinforcements in the matrix (Chen et al. 2016; Baron et al. 2016). In recent years, iron based alloys and steels have also been widely researched as matrix owing to their low cost, availability and adequate mechanical properties. However, austenitic stainless steels are susceptible to many common forms of wear and friction damage due to their low hardness which limits their application in tribological environment (Sulima et al.2016). A promising pathway to overcome this deficiency is the introduction of suitable hard ceramic particles. Steel matrix composites can be more viable in their application by improving the properties and finding more economical synthesis techniques. Thus the requirement of low cost along with enhanced toughness and wear resistance has led to significant interest in development of ceramic reinforced steel matrix composites. However, in order to achieve the desired properties, proper choice of sintering condition, nature of reinforcement, size and content of reinforcements are very crucial. Literature shows an increase in wear resistance of MMCs with increase in the volume fraction of reinforcement (Moazami-Goudarzi and Akhlaghi 2016; Jin et al.2017; Chi et al.2015). Ease of processing and affordability could provide a greater scope for potential

1
2
3 application of steel matrix composites, and thus various types of reinforcements are being
4
5 incorporated by the researcher to realise this objective.
6

7 In this direction, TiB₂ as reinforcement in steel matrix has received lot of attention
8 recently. This can be attributed to unique properties of TiB₂ such as low density (4.5 g/cc),
9 high melting point (3225 °C), high elastic modulus (430 GPa), high hardness (~32 GPa),
10 good abrasion resistance and good wettability and stability in steel matrix (Sulima et al.2011;
11 Wang et al.2013). These excellent properties make it attractive for many high performance
12 structural applications such as cutting tools, crucibles, wear resistance and corrosion
13 resistance parts. Although, several methods for fabrication of steel matrix composites are
14 known (Yang et al.2009; Zhang et al.2007; Pagounis and Lindroos 1998; Lepakova et
15 al.2004), homogeneous distribution of reinforcement still remains a challenge and efforts
16 needed to address this issue. Powder processing route is considered as economically viable
17 and attractive route for the synthesis of particle reinforced MMCs owing to less reactivity
18 between matrix and reinforcement. Also, powder metallurgy route allows for wide range of
19 reinforcement with higher content (Bains et al.2016). Although a variety of powder
20 metallurgy based approaches have been developed to synthesize these types of composites to
21 obtain excellent combination of the properties, little research has been done to understand the
22 strengthening mechanisms in TiB₂ reinforced steel matrix composites (Wang et al.2006;
23 Sulima et al.2014; Tjong and Lau 2000). Sulima et al. (2014) reported a minimum friction
24 coefficient (0.32) and specific wear rate (208x10⁻⁶) for composite containing 8 vol.% TiB₂
25 and sintered at 1300 °C by spark plasma method. In another work, similar enhancement of
26 wear resistance was observed in AISI 316L stainless steel reinforced with 8 vol.% TiB₂
27 particles prepared by high pressure-high temperature (HP-HT) method (Sulima et al. 2014).
28 Tjong and Lau .(1999) reported improvement of the wear resistance of AISI 304 stainless
29 steel reinforced with 20 vol.% TiB₂ particles synthesized by hot isostatic pressing (HIP).
30
31
32
33
34
35
36
37
38
39
40
41
42
43
44
45
46
47
48
49
50
51
52
53
54
55
56
57
58
59
60

1
2
3 They also observed decrease in volumetric wear of the composite with increasing applied
4 normal loads or with sliding velocity.
5
6

7 It is apparent that despite extensive research on synthesis by HT-HP, HIPing, SPS, attempts
8 to synthesize steel matrix by hot pressing method is not reported. Hot pressing method is a
9 cost effective powder metallurgy route along with extensive applications in industries. In
10 addition, this method ensures uniform distribution of particles in the matrix and thus
11 contributing to the enhancement in the strength. In light of these facts, we speculate
12 fabrication of steel matrix composite by hot pressing route would not only be economical as
13 compared to existing powder metallurgy routes but also enhance its potential in many
14 advanced applications. Therefore, the current work is intended to study the influence of TiB_2
15 and hot pressing sintering temperature on mechanical and wear properties of the hot pressed
16 composites. In addition, the possible strengthening mechanisms operating for enhancement in
17 strength of these composites are also be explored.
18
19
20
21
22
23
24
25
26
27
28
29
30

31 **2. Materials and methods**

32
33 In the present investigation, commercially available AISI 304 Stainless Steel (AISI 304 SS)
34 powder with an average particle size of 28 μm supplied by Nanoshell, India was used as the
35 matrix and the chemical composition is shown in Table 1. TiB_2 powders with an average
36 particle size of 2 μm was used as reinforcement (Subramanian et al.2007). To achieve
37 homogeneous mixing, steel powder and TiB_2 powder (2 vol.% and 4 vol.%) were mixed in a
38 high energy ball mill (Model: PM-400) for 2 hours. Then the resulting mixed powders were
39 loaded in a graphite die having inner diameter 30 mm. Thereafter, consolidation of mixed
40 powders were done by uniaxial vacuum hot pressing (Vacuum Tech Pvt. Ltd., India) at 1000
41 $^\circ\text{C}$ and 1100 $^\circ\text{C}$ with heating rate of 25 $^\circ\text{C}/\text{min}$ for 15 minutes at 48 MPa pressure. Finally,
42 disc shaped compacts with diameter 30 mm and thickness 3 mm were sectioned.
43
44
45
46
47
48
49
50
51
52
53
54
55
56
57
58
59
60

1
2
3 The densities of the hot pressed compacts were estimated by Archimedes water
4 immersion method. Relative density was evaluated from theoretical absolute density and
5 experimentally observed density. The theoretical densities of the resultant composites were
6 calculated following the rule of mixtures, considering the theoretical densities for steel and
7 TiB₂ as 7.9 gm/cm³ and 4.5 gm/cm³ respectively (Sulima et al. 2014). For metallographic
8 study, the hot pressed compacts were sectioned and polished as per standard procedure.
9 Microstructural assessment of the samples was then conducted using Scanning Electron
10 Microscope (SEM) (Model: Zeiss EVO18) equipped with Energy Dispersive X-ray
11 spectroscopy (EDS) for chemical microanalysis. Distribution of elements in the matrix was
12 analysed by conducting EDX attached with SEM.
13
14
15
16
17
18
19
20
21
22
23

24 Vickers indentation tests (HV0.1) was carried out on polished surface of the hot
25 pressed samples using a 136⁰ Vicker diamond pyramid indenter under a load of 0.98 N (100
26 gf) at room temperature. Compression test was performed in order to investigate the behavior
27 of the synthesized composites with different volume fractions of TiB₂ under the influence of
28 compressive load. The compression test samples were sectioned from hot pressed compact in
29 cylindrical shape having a diameter of 2.5 mm and height of 5 mm as per ASTM standard.
30 The compression test was carried out by using a servo hydraulic universal testing machine
31 (INSTRON 8801) with a constant strain rate of 1 mm/min. at room temperature. A
32 photograph of testing machine and schematic picture of compressive sample is shown in
33 Figure 1a and b. Four compression tests were conducted for each sample for analysing the
34 results and compressive yield strength was reported by taking the average of these four
35 results. Wear test was conducted in order to study the tribological performance of the
36 synthesized composites as a function of TiB₂ content. Dry sliding wear test was performed by
37 block-on-disc method using multiple tribo Tester (Model: TR-25, DUCOM, Bangalore) on
38 prepared composite specimens at sliding speed 0.3 m/s with normal load of 35 N. The
39
40
41
42
43
44
45
46
47
48
49
50
51
52
53
54
55
56
57
58
59
60

counter wheel material was made of EN 31 steel coated with titanium aluminium nitride (TiAlN). A block of size 9 mm x 6.5 mm x 3 mm machined from the synthesized composite for wear testing as per ASTM G 77-98 standard. Before testing, the flat surface of the specimens was polished to achieve uniform surface finish. Wear tests were carried out at room temperature without lubrication for 30 min. Wear of specimen in terms of wear depth and coefficient of friction was recorded automatically during the tests.

3. Results and discussion

3.1 Microstructure

Figure 2 shows the SEM micrograph of hot pressed unreinforced steel matrix along with total area EDX analysis. EDX results confirmed the presence of Fe, Cr, Ni as main elements without presence of any foreign elements. Figure 3 gives the SEM micrograph of composite with 2 vol.% TiB₂ with EDX results at the indicated points. As shown in Figure 3, point 1 presents TiB₂ (light grey colour) and point 2 presents matrix phase which can be supported by corresponding EDX results. Point 1 consists of Ti and B while point 2 consists of Fe, Cr, Ni etc. SEM micrograph also reveals relatively uniform distribution of TiB₂ along the grain boundary which contributes to enhanced mechanical properties. Figure 4 presents the SEM micrograph of composite with 4vol.% TiB₂ along with corresponding EDX mapping. The map shows the elemental distribution of Ti and B along with the parent matrix elements. The average reinforcement particle size was found to be in the range of 0.7-0.8 μm. Clustering of particles are also observed in some location in composite containing 4 vol.% TiB₂ (as shown in Figure 4 which is quite expected due to increase in volume fraction of fine reinforcement particles(Leszczynska-Madej et al.2017).

3.2 Density

The relative density of the investigated hot pressed samples is shown in Figure 5. The relative density of resultant composites range from 87 - 92% of theoretical density. The inconsistency

1
2
3 between theoretical and experimental values of density indicates presence of porosity. The
4 density of composite decreases from 7.10 to 6.91 when TiB₂ content increases from 2 vol.%
5 to 4 vol.% due to low density of TiB₂. Again, a significant difference in relative density can
6 be observed in the specimen pressed at 1000 °C and 1100 °C with same TiB₂ content. This
7 can be attributed to influence of temperature on solid state diffusion mechanism thereby
8 increasing sinterability and hence densification. Further, the more uniform distribution of TiB₂
9 particles in the matrix at high temperature as evident from microstructure can attenuate the
10 pinning effect of second phase particles and accordingly increase densification (Pagounis and
11 Lindroos 1998). Therefore, there is a need to optimize hot pressing parameters to maximize
12 densification.
13
14
15
16
17
18
19
20
21
22
23

24 **3.3 Hardness**

25
26 The results of microhardness tests of composites synthesized by hot pressing are shown in
27 Figure 6. It can be observed that hardness of steel matrix composite shows an increasing
28 trend with increasing amount of TiB₂ particles. This is due to presence of hard TiB₂ particles
29 in the matrix that results in constraint to plastic deformation of soft matrix during indentation.
30 For particle reinforced MMC, increasing the volume content of reinforcements results in a
31 low interparticle spacing and consequently leading to higher stresses for the passage of
32 dislocations through the hard ceramic phase for a given reinforcement particle size (Sulima et
33 al. 2014)). From Figure 6, it is evident that the hardness increases with increasing processing
34 temperature irrespective of TiB₂ content. This is due to higher densification of composite at
35 higher temperature and uniform distribution of particles along the grain boundary as evident
36 from the microstructure resulting in increased hardness. Sulima et al.(2014) reported similar
37 type of observation for steel matrix composites sintered by spark plasma process. Among the
38 samples investigated in the current study, steel matrix composite reinforced with 4 vol.%
39 TiB₂ hot pressed at 1100 °C exhibited highest hardness value as compared to other prepared
40
41
42
43
44
45
46
47
48
49
50
51
52
53
54
55
56
57
58
59
60

1
2
3 samples. It is interesting to note that amount of reinforcement phase determines the hardness
4 of composites in the present work rather than the porosity in the microstructure. This
5 observation could be attributed to high hardness value of TiB_2 and good interface bonding
6 between the particle and matrix. Further it is well known that introduction of hard ceramic
7 particles increases the strain energy by generation of dislocation due to difference in thermal
8 expansion coefficient between matrix and reinforcement thereby resulting high
9 hardness(Leszczynska-Madej et al.2017).
10
11
12
13
14
15
16
17

18 ***3.4 Compressive properties***

19
20 Typical compression behavior of hot pressed 304- TiB_2 composites is shown in Figure 7. The
21 compression strength of the composites are higher than unreinforced steel indicating positive
22 effect of TiB_2 reinforcement on the mechanical properties of steel. The compressive strength
23 increase at the expense of ductility. This finding can be ascribed to dominating role of TiB_2
24 for enhancement of compressive strength over deterioration effect of increased porosity. The
25 compressive yield strength of hot pressed steel matrix without reinforcement is in the range
26 of 945 - 1227 MPa. The compressive yield strength of the composites sintered at 1000 °C
27 with 2 vol.% of TiB_2 and 4 vol.% of TiB_2 content are 1124 MPa and 1279 MPa respectively.
28 However, the plastic deformation of the hotpressed samples decreases from 23% for the
29 unreinforced steel to 18% for the composites with 2 vol.% of TiB_2 and to 15% for the
30 composites with 4 vol.% of TiB_2 . Lowering of ductility is due to presence of TiB_2 that
31 prevents the plastic deformation and blocks the dislocation motion. Comparing Figure 7a and
32 b, an increase in strength of the composites can be observed with increase in processing
33 temperature. The ultimate compressive yield strength of hot pressed steel matrix without
34 reinforcement increases from 945 MPa (sintered at 1000 °C) to 1227 MPa (sintered at 1100
35 °C). Therefore it is also noteworthy that samples pressed at 1100 °C exhibited notably high
36 strength as compared to samples hot pressed at 1000 °C which can be attributed to their low
37
38
39
40
41
42
43
44
45
46
47
48
49
50
51
52
53
54
55
56
57
58
59
60

1
2
3 porosity and adequate bonding between the particles. Based on the results, it is clear that the
4
5 compressive yield strength increased with increasing processing temperature indicating
6
7 significant relationship between processing temperature and mechanical properties. It is also
8
9 confirmed that strength of the reinforced steel matrix has not deteriorated despite the
10
11 presence of porosity.
12

13 **3.4.1. Strengthening mechanisms**

14
15 Several mechanisms and models have been recommended in order to provide more insight
16
17 towards the enhancement of strength of metal matrix composites. Such as (a) Load transfer
18
19 from the matrix to the reinforcement particle at the interface (shear lag model) (b) Increased
20
21 dislocation densities produced on cooling due to large difference in coefficient of thermal
22
23 expansion (CTE) of the matrix and that of the reinforcement particles (Taylor strengthening)
24
25 (c) Orowan strengthening due to artificially reduction in inter particle spacing (d) Work
26
27 hardening due to presence of hard ceramic particles (Asl and Kakroudi 2015). All the above
28
29 said mechanisms are expected to be suitable for steel matrix composites synthesized in the
30
31 present work.
32
33

34
35 First, the relation between dislocation density and strengthening has long been established by
36
37 many researchers (Chelliah et al.2017).When a metal matrix composite is subjected to
38
39 temperature change, dislocations are generated in the vicinity of ceramic reinforcement due
40
41 to difference in coefficient of thermal expansion (CTE) between matrix and reinforcement so
42
43 as to reduce the stored energy. In the present work, all the fabricated samples are imposed to
44
45 temperature difference of 975 °C for processed at 1000 °C and 1075 °C for processed at 1100
46
47 °C. Again, the difference in CTE between steel matrix and TiB₂ particle is $10 \times 10^{-6}/K$ which
48
49 can lead to generation of geometrically necessary dislocations in order to accommodate this
50
51 thermal mismatch. The increment in the yield strength due to generation of dislocation owing
52
53
54
55
56
57
58
59
60

to relaxation of thermal mismatch or Taylor strengthening can be expressed as (Zhang and Chen 2006):

$$\Delta\sigma_{CTE} = \beta G_m b \sqrt{\frac{12\Delta\alpha\Delta T V_p}{b d_p (1-V_p)}} \quad (1)$$

Where β is strengthening coefficient, G_m is shear modulus of the matrix, b is Burgers vector, $\Delta\alpha$ is the difference of CTE between steel matrix and TiB₂ particles, ΔT is the difference between the processing and test temperature, V_p and d_p present the volume fraction and average particle size of TiB₂ reinforcements.

Another aspect that can contribute to the enhancement of strength is Orowan strengthening from dispersoids present in the matrix. The Orowan strengthening model describes improvements in strength in the matrix material due to formation of dislocation loops around the particles (Zhang and Chen 2006). It is generally believed that the Orowan strengthening mechanism is not significant for metal matrix composites reinforced with a particle size greater than 5 micron (Xiao et al.2018). In the present work, average particle size of the reinforcement is in submicron range (0.7-0.8 μm) indicating Orowan strengthening can contribute slightly to the improvement of yield strength of composites (Nie et al.2017). The contribution of Orowan strengthening in MMC increases with increase in volume fraction of reinforcement particles and decrease in interparticle spacing between dispersoids which impedes the movement of dislocation (Chelliah et al.2017). Increment of yield strength due to Orowan strengthening can be described by the following expression below: (Nie et al.2017).

$$\Delta\sigma_{orowan} = \frac{0.13 G_m b}{d_p \left[(1/2V_p)^{\frac{1}{3}} - 1 \right]} \ln \left(\frac{d_p}{2b} \right) \quad (2)$$

In addition, the load transfer strengthening mechanism can be used to explain the improvement of yield strength of the composites due to load bearing effect of hard ceramic phase. It is reported that the good interfacial bonding between dispersed particles and matrix

1
2
3 contributes to better transfer of the applied load to the reinforcement. The enhancement of
4 strength due to load transfer effect can be described by (Dai et al.2001)

$$\Delta\sigma_{Load} = 0.5V_p\sigma_m \quad (3)$$

7
8 Where σ_m is the yield strength of matrix and V_p is the volume fraction of TiB₂ particles.

9
10 The parameters and properties used for calculating the improvement in yield strength of the
11 composites by various strengthening mechanisms are listed in Table 2.

12
13 Based on above governing equations for different strengthening mechanisms, the
14 enhancement of yield strength of the composites with different content of TiB₂ and
15 processing temperature was calculated and shown in Figure 8. It can be seen that contribution
16 due to thermal mismatch strengthening mechanism plays a significant role towards
17 enhancement of strength as compared to other strengthening mechanisms. The predominance
18 effect of thermal mismatch strengthening can be attributed to large difference in temperature
19 and coefficient of thermal expansion that increases the magnitude of thermal strain ($\Delta\epsilon_T =$
20 $\Delta\alpha\Delta T$) and density of geometric dislocation. In Figure 8a and b, dislocation strengthening in
21 the composites show an increasing trend with increase in TiB₂ content and processing
22 temperature. Further, it can be noticed that load transfer strengthening contributed slightly
23 due to low volume fraction of TiB₂ in the current work. The observed results also reveal the
24 relative contribution of Orowan strengthening in composite with 4 vol.% TiB₂ is increased by
25 1.45 times as compared to composite with 2 vol.% TiB₂. This observation can be attributed to
26 decrease in interparticle distance with increase in TiB₂ resulting in enhanced pinning effect
27 and more restriction of plastic flow of the matrix and improved strength. However based on
28 the above results, we can conclude that Taylor strengthening due to thermal mismatch plays
29 as most dominating strengthening mechanism compared to others.

30
31 Several numerical models are available for estimation of theoretical yield strength of particle
32 reinforced MMCs. Among these methods, modified Zhang and Chen model and summation
33
34
35
36
37
38
39
40
41
42
43
44
45
46
47
48
49
50
51

models are commonly used to predict the yield strength of particle reinforced MMCs (Zhang Z and Chen 2006; Xiao et al.2018; Frost and Ashby1982). Zhang and Chen model is based on the assumption of interdependent relationship between individual strengthening mechanisms. This model includes the effect of Orowan strengthening, thermal mismatch strengthening and load bearing. The theoretical increase in yield strength by this model can be expressed as follows:

$$\Delta\sigma_{ZC} = (1 + 0.5V_p) \left[\sigma_{ym} + \Delta\sigma_{Orowan} + \Delta\sigma_{Taylor} + \left(\frac{\Delta\sigma_{Orowan}\Delta\sigma_{Taylor}}{\sigma_{ym}} \right) \right] \quad (4)$$

On the other hand, summation model considers all the strengthening contribution acting individually on the materials. The theoretical increase in yield strength by this model can be described by:

$$\Delta\sigma_S = \sigma_{ym} + \Delta\sigma_{Orowan} + \Delta\sigma_{Taylor} + \Delta\sigma_{Load} \quad (5)$$

Figure 9 presents a comparison between the experimental values of yield strength of composites and theoretical values estimated by Zhang and Chen model and summation model. Figure 9a and b also confirms the improvement of strength with increase in TiB₂ content and processing temperature. The estimated yield strength from model approximates the experimental values. The experimental yield strength is higher than the model values indicating contribution of other strengthening mechanisms. Thus it is clearly evident that existence of particle and particle size distribution should be considered for enhancement of strength.

3.5 Elastic modulus

Elastic modulus of particle reinforced composites can be calculated using the simple rule-of mixtures (ROM) (Kim et al.2013).

$$\text{Under iso-strain condition, } E_C = E_p V_p + E_m V_m \quad (6)$$

$$\text{Under iso-stress condition, } E_C = \frac{E_p E_m}{E_p V_m + E_m V_p} \quad (7)$$

Where V_p stands for volume percentage of TiB_2 particulate, V_m stands for the volume fraction of matrix, E_p is the elastic modulus of TiB_2 particulate, and E_m is the elastic modulus of matrix.

However, effective modulus of particulate composites can be evaluated by Halpin–Tsai (HT) model (Reddy and Zitoun 2011) that takes into account the aspect ratio of the reinforcements in addition to the volume fraction and elastic modulus of the reinforcements and matrix and is expressed as

$$E_c = \frac{E_m(1+2sqV_p)}{1-qV_p} \quad (8)$$

where E_c and E_m present the Young's moduli of the composite and the matrix respectively, s is the aspect ratio of the reinforcement, V_p is the volume fraction, and q is a geometrical parameter that can be written as

$$q = \frac{\left(\frac{E_p}{E_m}\right)^{-1}}{\left(\frac{E_p}{E_m}\right)^{-1} + 2s} \quad (9)$$

Substituting the values of elastic modulus of steel as 193 GPa and elastic modulus of TiB_2 as 430 GPa (Sulima et al.2011) in equations (6) to (9), elastic modulus for composites with different content of TiB_2 are calculated. Comparative analysis between estimated values of elastic modulus and the experimental value is presented in Figure 10. The experimental values matches well with the values estimated by HT model and ROM. The experimental results indicate a significant improvement in elastic modulus of the composite with 4 vol.% TiB_2 particles. This remarkable improvement in the elastic modulus of the composites can be mainly attributed to high elastic modulus of reinforcing TiB_2 particle and homogeneous distribution of reinforcement particles in the matrix. In addition, increase in interfacial area with increase in volume fraction of reinforcement particles enhances the stress transfer from plastically deforming ductile metal matrix to hard, brittle reinforcing particles. It is also

1
2
3 evident that experimental value of elastic modulus of unreinforced steel is lower than the
4
5 theoretical value which can be ascribed to lower relative density of the sample.
6

7 **3.6 Wear properties**

8
9 Wear behavior of material can be expressed by depth of wear that indicates removal of
10
11 material from the surface. Figure 11 shows wear depth curves of unreinforced steel matrix
12
13 and composite reinforced with 2 vol.%, 4 vol.% TiB₂ sintered at 1000 °C and 1100 °C. It is
14
15 apparent that depth of wear approaches a steady state wear regime within few seconds of
16
17 commencement of the test. The depth of wear of composites is low as compared to
18
19 unreinforced steel. Also, depth of wear decreases with increase in volume percentage of TiB₂
20
21 indicating enhanced wear performance. This enhancement can be attributed to increased
22
23 hardness and strength due to presence of higher amount of hard TiB₂ particles. The higher
24
25 amount of TiB₂ particles increases the load carrying capacity and resistance to plastic
26
27 deformation by impeding dislocation motion. It has been reported that particles are the most
28
29 effective in improving the wear resistance of MMCs (Moazami-Goudarzi and Akhlaghi 2016;
30
31 Jin et al.2017; Chi et al.2015; Jin et al.2017). It is well known that hardness of MMCs
32
33 increases with increase in amount of reinforcement particles thereby significantly influencing
34
35 the wear resistance by decreasing in real area of wear surface. Reports of earlier research on
36
37 wear behavior of particle reinforced MMCs demonstrated the dependence of wear resistance
38
39 on hardness as well as mean free path between the reinforced particles. In general, wear
40
41 resistance is proportional to H/λ (Jin et al.2017) where H represents hardness and λ
42
43 represents mean free path. Literature suggests that interparticle spacing plays an important
44
45 role in wear resistance of composites. It depends on the reinforcement particle size d and the
46
47 volume fraction f by the expression as
48
49
50
51

$$52 \lambda \propto d/\sqrt{f} \quad (10)$$

53
54
55
56
57
58
59
60

1
2
3 This expression predicts shorter mean free path for higher volume fraction of reinforcement
4 particles. According to the present results, wear resistance of the 4 vol.% TiB₂/steel
5 composite is higher as compared to 2 vol.%TiB₂/steel composites. Based on the above
6 results, it is reasonable to assume that wear resistance of the present composites is improved
7 due to decrease in λ owing to increase in TiB₂ content. Decrease in λ results in reduction of
8 indentation depth of soft abrasive particles with almost no significant grooves. Similar
9 tendency of increase of wear response and hardness was reported by Tjong and Lau (2000)
10 and Sulima et al. (2014) for TiB₂ reinforced steel MMCs synthesized by powder metallurgy
11 methods. Mahajan et al. (2015) investigated the influence of wettability on the wear behavior
12 of composite. They reported good bonding between matrix and reinforcement ensures
13 improved wear resistance. So observation of steady state wear regime in our results confirm
14 the good bonding between TiB₂ particles and steel matrix. The present results indicate
15 decrease in depth of wear of the samples with increase in hot pressing temperature as shown
16 in Figure 11b. This is quite obvious because increase in sintering temperature in the present
17 case enhances the hardness as compared to composites sintered at lower temperature. This
18 finding is in support of Archard's wear law which suggests an inverse relationship between
19 hardness and wear rate. As far as the wear behavior of composites is concerned, it is
20 influenced by microstructural properties and nature of reinforcement. Composites sintered at
21 higher temperature were accompanied with higher density that leads to lower wear depth due
22 to a reduced amount of loss of adherence of particles. Another suggested reason for
23 enhancement of wear performance is uniform distribution of reinforcement particles in the
24 matrix as evident in the microstructure. Present results are consistent with investigations of
25 Sulima et al.(2014) who reported similar variation of wear behavior with sintering
26 temperature for steel matrix composites containing 4 and 8 vol. % TiB₂ fabricated by SPS
27 process. Hence, it is worth to state that addition of TiB₂ reinforcements are most effective for
28
29
30
31
32
33
34
35
36
37
38
39
40
41
42
43
44
45
46
47
48
49
50
51
52
53
54
55
56
57
58
59
60

1
2
3 enhancement of wear performance of steel matrix composites as compared to unreinforced
4
5 steel.

6
7 Figure 12 shows coefficient of friction (COF) of the specimens with test duration at an
8
9 applied load of 35 N and a sliding speed 0.3 m/s. It is very evident from the Figure 12 that
10
11 COF values are almost steady with testing time indicating minimal damage due to
12
13 dominating role of TiB₂ to sliding behavior at this load. It can be seen that variation of
14
15 coefficient friction has a similar trend as that for depth of wear. The COF decreases with the
16
17 increase of TiB₂ content. Average value of COF of the unreinforced steel sintered at 1000 °C
18
19 is in the range of 0.37-0.51 whereas that of composites reinforced with 2 vol.% and 4 vol.%
20
21 TiB₂ are in the range of 0.29-0.40 and 0.28-0.31 respectively. The influence of TiB₂ on
22
23 tribological properties of composites can be clearly observed from the graph. This observed
24
25 variation in COF depending upon reinforcement content can be explained by degree of plastic
26
27 deformation. The simplified theory of friction proposed by Bowdon and Tabor is given by the
28
29 following relation (Chelliah et al.2016):
30
31

$$\mu = \tau_i / 2.8Y \quad (11)$$

32
33 where μ stand for coefficient of friction, τ_i stands for shear strength and Y represents flow
34
35 pressure or hardness of the material. This equation represents an inverse relationship between
36
37 hardness and coefficient of friction. Materials exhibits lower μ with higher hardness due to
38
39 minimal degree of plastic deformation. In the present investigation, it is apparent that
40
41 composites with 4 vol.% TiB₂ results in higher hardness as compared to other samples.
42
43 Hence, it can be concluded that higher amount of TiB₂ provide more protection to steel
44
45 matrix during sliding by inhibiting plastic deformation and delaying material removal from
46
47 the surface. Furthermore, the results revealed the dependence of the friction coefficient of the
48
49 composites on the sintering temperature with the same content of TiB₂ particles as shown in
50
51 Figure 12b. It is interesting to note that application of higher sintering temperature play a
52
53
54
55
56
57
58
59
60

1
2
3 remarkable role in improving the wear behavior of sintered composites with the same content
4 of TiB₂. Coefficient of friction values of unreinforced steel decreases from 0.51 to 0.46 with
5 increase in temperature from 1000 °C to 1100 °C. The lowest value of the coefficient friction
6 was obtained in composite with 4 vol.% of TiB₂ sintered at 1100 °C as compared to sintered
7 at 1000 °C. In the case of composites with 2 vol.% TiB₂, the friction coefficient is 0.40 for
8 sintering temperature of 1000 °C and reduces gradually to 0.34 at sintering temperature of
9 1100 °C. Based on these results, it can be clearly seen that sintering temperature acts as
10 another influential parameter for control of wear performance of composites irrespective of
11 content of TiB₂ particles in the matrix. Higher sintering temperature favours more
12 homogeneous distribution of the fine reinforcements as shown in Figure 4 which results in
13 enhancement of wear resistance due to increase in load bearing capacity by reducing the
14 contact area between specimen and counterpart. Moreover, based on the Archard's equation,
15 wear performance of composites increases with the increased hardness, by increasing the
16 resistance of material to plastic deformation. Similar trend in variation of COF with respect to
17 reinforcement content and sintering temperature have been also reported by other researchers
18 in previous studies (Sulima 2014; Tjong and Lau .1999; Chelliah et al.2016;Sulima et
19 al.2016). Thus it can be concluded that incorporation of TiB₂ particles into steel matrix
20 enhances the wear performance effectively.

41 **4. Conclusions**

42 The following are the major findings based on microstructure, mechanical properties and
43 wear behavior of steel matrix composites reinforced with 2 and 4 vol.% TiB₂ particles
44 synthesized by hot pressing method:
45
46
47
48
49

- 50 (a) At lower fractions, TiB₂ is uniformly distributed within the steel matrix while few
51 clustering is observed at higher fractions of TiB₂. Optimization of the process
52 parameters is necessary in order to achieve higher densification level.
53
54
55
56
57

- 1
2
3 (b) Steel matrix composites reinforced with TiB_2 particles exhibited high hardness,
4 ultimate compressive strength, elastic modulus and yield strength as compared to
5 their unreinforced counterpart. Hardness of the composites reinforced with 2 vol.%
6 TiB_2 and 4 vol.% TiB_2 was improved by 30% and 42% respectively than that of
7 unreinforced steel sintered at 1100 °C.
8
9
10
11
12
13 (c) Taylor strengthening caused due to large difference in CTE and temperature change
14 is the major contributor in strengthening these composites. This is followed by
15 Orowan strengthening and load bearing strengthening.
16
17
18
19
20 (d) The results of wear tests revealed decrease in depth of wear and COF with increase in
21 the content of TiB_2 . The composite with 4 vol.% TiB_2 sintered at 1100 °C showed the
22 best wear resistance.
23
24
25

26 **Funding**

27
28 The work was supported by the Board of Research in Nuclear Science (BRNS) of the
29 Department of Atomic Energy (DAE), Government of India (No. 36(2)/14/18/2016- BRNS).
30
31
32
33
34
35
36
37
38
39
40
41
42
43
44
45
46
47
48
49
50
51
52
53
54
55
56
57
58
59
60

References

- Akhtar, F. 2014. Ceramic reinforced high modulus steel composites: processing, microstructure and properties. *Canadian Metallurgical Quarterly* 53: 253-263. doi:10.1179/1879139514Y.0000000135.
- Asl, M.S., and M.G. Kakroudi. 2015. A Processing–Microstructure Correlation in ZrB₂–SiC Composites Hot-pressed under a Load of 10 MPa. *Universal Journal of Material Science* 3: 14-21. doi:10.13189/ujms.2015.030103.
- Bains, P. S., S.S. Sidhu, and H.S. Payal. 2016. Fabrication and Machining of Metal Matrix Composites: A Review. *Materials and Manufacturing Processes* 31: 553-573. doi:10.1080/10426914.2015.1025976.
- Baron, C., H. Springer, and D. Raabe. 2016. Efficient liquid metallurgy synthesis of Fe-TiB₂ high modulus steels via in-situ reduction of titanium oxides. *Materials and Design* 97: 357-363. doi:10.1016/j.matdes.2016.02.076.
- Chen, S., Z. Zhao, X. Huang, and L. Zhang. 2016. Interfacial microstructure and mechanical properties of laminated composites of TiB₂-based ceramic and 42CrMo alloy steel. *Material Science and Engineering A* 674: 335–342. doi:10.1016/j.msea.2016.07.106.
- Chelliah, N. M., H. Singh, and M K. Surappa. 2017. Microstructural evolution and strengthening behavior in in-situ magnesium matrix composites fabricated by solidification processing. *Materials Chemistry and Physics* 194: 65-76. doi: 10.1016/j.matchemphys.2017.03.025.
- Chi. H., L. Jianga, G. Chena, P. Kang, X. Lin, and G.Wu. 2015. Dry sliding friction and wear behavior of (TiB₂+h-BN)/2024Al composites. *Materials and Design* 87; 960–968. doi:10.1016/j.matdes.2015.08.088.
- Dai, L.H., Z. Ling and Y.L. Bai. 2001. Size-dependent inelastic behavior of particle-reinforced metal–matrix composites. *Composite Science and Technology* 61:1057-1063. doi: 10.1016/S0266-3538(00)00235-9.
- Frost, H.J., and M.F. Ashby. 1982. Deformation-Mechanism Maps, The Plasticity and Creep of Metals and Ceramics. 1st ed. New york: Pergamon.
- Jayakumar, K., J. Mathew, M.A. Joseph, R.K.Suresh, A.K. Shukla, and M.G. Samuel. 2013. Synthesis and Characterization of A356-SiC_p Composite produced through Vacuum Hot Pressing. *Materials and Manufacturing Processes* 28: 991–998. doi:0.1080/10426914.2013.773012.
- Jin, C., C.C. Onuoha, Z. N. Farhat, G. J. Kipouros, and K. P. Plucknett. 2017. Reciprocating wear behavior of TiC-stainless steel cermets. *Tribology International* 105: 250–263. doi:10.1016/j.triboint.2016.10.012.

- 1
2
3 Kim, C.S., Sohn II, Nezafati M, B. Ferguson, B. F. Schultz, Z.B. Gohari Pradeep, K. Rohatgi, and K. Cho. 2013.
4 Prediction models for the yield strength of particle-reinforced unimodal pure magnesium (Mg) metal matrix
5 nanocomposites (MMNCs). *Journal of Material Science* 48: 4191-4204. doi: 10.1007/s10853-013-7232-x.
6
7
8 Lepakova, O. K., L. J. Raskolenko, and Y. M. Maksimov. 2004. Self-propagating high-temperature synthesis of
9 composite material Titanium diboride-Fe. *Journal of Material Science* 39: 3723 - 3732.
10
11
12 Leszczyńska-Madej, B., A. Wąsik, and M. Madej. 2017 Microstructure characterization of SiC reinforced
13 aluminium and Al₄Cu alloy matrix composites. *Archives of Metallurgy and Materials* 62: 747-755.
14
15 doi: 10.1515/amm-2017-0112.
16
17 Mahajan, G., N. Karve, U. Patil, P. Kuppan, and K. Venkatesan. 2015. Analysis of Microstructure, Hardness
18 and Wear of Al-SiC-TiB₂ Hybrid Metal Matrix Composite. *Indian Journal of Science and Technology* 8:
19 101-105. doi: 10.17485/ijst/2015/v8iS2/59081.
20
21
22 Moazami-Goudarzi, M., and F. Akhlaghi. 2016. Wear behavior of Al 5252 alloy reinforced with micrometric
23 and nanometric SiC particles. *Tribology International* 102: 28–37. doi:10.1016/j.triboint.2016.05.013.
24
25
26 Nie, K., K. Deng, X. Wang, and K. Wu. 2017. Characterization and strengthening mechanism of SiC
27 nanoparticles reinforced magnesium matrix composite fabricated by ultrasonic vibration assisted squeeze
28 casting. *Journal of Materials Research* 32: 2609-2620. doi:10.1557/jmr.2017.202.
29
30
31
32 Pagounis, E., and V. K. Lindroos. 1998. Processing and properties of particulate reinforced steel matrix
33 composites. *Material Science and Engineering A* 246: 221- 234. doi:10.1016/S0921-5093(97)00710-7.
34
35
36 Rana, R. and C. Liu. 2014. Effects of ceramic particles and composition on elastic modulus of low density steels
37 for automotive applications. *Canadian Metallurgical Quarterly* 53: 300-316.
38
39 doi:10.1179/1879139514Y.0000000130.
40
41
42 Reddy, A.C., and E. Zitoun. 2011. Strengthening mechanisms and fracture behavior of 7072Al/Al₂O₃ metal
43 matrix Composites. *International Journal of Engineering Science and Technology* 3: 6090-6100.
44
45
46 Sanaty-Zadeh, A., and P.K. Rohatgi. 2012. Comparison between current models for the strength of particulate-
47 reinforced metal matrix nanocomposites with emphasis on consideration of Hall-Petch effect. *Material*
48 *Science and Engineering A* 531: 112-118. doi:10.1016/j.msea.2011.10.043.
49
50
51 Springer, H., R. Aparicio Fernandez, M. J. Duarte, A. Kostka, and D. Raabe. 2015. Microstructure refinement
52 for high modulus in-situ metal matrix composite steels via controlled solidification of the system Fe-TiB₂.
53
54 *Acta Materialia* 96: 47–56. doi:10.1016/j.actamat.2015.06.017.
55
56
57
58
59
60

- 1
2
3 Subramanian, C., T.S.R.Ch. Murthy, and A.K. Suri.2007.Synthesis and consolidation of titanium diboride.
4
5 *International Journal of Refractory Metals & Hard Materials* 25:345-350.doi:10.1016/j.ijrmhm.2006.09.003
6
7 Sulima, I., L. Jaworska, P. Wyżga, and M. Perek-Nowak. 2011. The influence of reinforcing particles on
8
9 mechanical and tribological properties and microstructure of the steel- Titanium diboride composites.
10
11 *Journal of Achievements Materials and Manufacturing Engineering* 48: 52-57.http://www.journalamme.org.
12
13 Sulima, I. 2014. Tribological properties of steel/ TiB₂ composites prepared by spark plasma sintering. *Archives*
14
15 *of Metallurgy and Materials* 59: 1263-1268.doi:10.2478/amm-2014-0216.
16
17 Sulima, I., L. Jaworska, and P. Figiel. 2014. Influence of processing parameters and different content of
18
19 Titanium diboride ceramics on the properties of composites sintered by high pressure - high temperature
20
21 (HP-HT) method. *Archeves of Metallurgy and Materials* 59: 205-209.doi: 10.2478/amm-2014-0033.
22
23 Sulima, I., P. Hyjek, and T. Tokarski. 2014. Influence of annealing conditions on the properties and
24
25 microstructure of steel composites. *Metal Foundry Engineering* 40: 33–43.doi:10.7949/mafe.2014.40.1.33.
26
27 Sulima, I., S. Boczkal, and L. Jaworska. 2016. SEM and TEM characterization of microstructure of stainless
28
29 steel composites reinforced with TiB₂. *Material Characterization* 118: 560-569.
30
31 doi:10.1016/j.matchar.2016.07.005.
32
33 Sulima, I., R. Kowalik, and P. Hyjek. 2016. The corrosion and mechanical properties of spark plasma sintered
34
35 composites reinforced with titanium diboride. *Journal of Alloys Compound* 688: 1195-1205.
36
37 doi:10.1016/j.jallcom.2016.07.132.
38
39 Tjong, S.C., and K.C. Lau. 2000. Abrasion resistance of stainless-steel composites reinforced with hard
40
41 Titanium diboride particles. *Composite Science and Technology* 60: 1141–1146.
42
43 doi:10.1016/S0266-3538(00)00008-7.
44
45 Tjong, S.C., and K. C. Lau. 1999. Sliding wear of stainless steel matrix composite reinforced with Titanium
46
47 diboride particles. *Materials Letters* 41: 153–158.doi: 10.1016/S0167-577X(99)00123-8.
48
49 Wang, X.H., M.Zhang, and B.S. Du. 2013. Fabrication of Multiple Ceramic Particle Reinforced Iron Matrix
50
51 Coating by Laser Cladding. *Materials and Manufacturing Processes* 28: 509–513.
52
53 doi:10.1080/10426914.2012.700154.
54
55 Wang, Y., Z. Q. Zhang, H. Y. Wang, B.X. Ma, and Q.C. Jiang. 2006. Effect of Fe content in Fe–Ti–B system on
56
57 fabricating Titanium diboride particulate locally reinforced steel matrix composites. *Material Science and*
58
59 *Engineering A* 422: 339–345. doi: 10.1016/j.msea.2006.02.012
60

- 1
2
3 Xiao, P., Y. Gao, C. Yang, Z. Liu, Y. Li, and F. Xu. 2018. Microstructure, mechanical properties and
4 strengthening mechanisms of Mg matrix composites reinforced with in situ nanosized TiB₂ particles.
5
6 *Material Science and Engineering A* 710: 251–259. doi:10.1016/j.msea.2017.10.107.
7
8 Yang, Y.F., H.Y. Wang, RY. Zhao, and Q. C. Jiang. 2009. In Situ TiC/TiB₂ Particulate Locally Reinforced Steel
9 Matrix Composites Fabricated Via the SHS Reaction of Ni–Ti–B₄C System. *International Journal of Applied*
10 *Ceramic Technology* 6: 437–446. doi: 10.1111/j.1744-7402.2008.02282.x.
11
12 Zhang, Z., P. Shen, Y. Wang, and Q. C. Jiang. 2007. Fabrication of TiC and Titanium diboride locally reinforced
13 steel matrix composites using a Fe–Ti–B₄C–C system by an SHS-casting route. *Journal of Material Science*
14 42: 8350–8356. doi:10.1007/s10853-006-0764-6.
15
16 Zhang, Z., and D.L. Chen. 2006. Consideration of Orowan strengthening effect in particulate reinforced metal
17 matrix nanocomposites: a model for predicting their yield strength. *Scripta Materialia* 54: 1321–1326.
18
19 doi:10.1016/j.scriptamat.2005.12.017.
20
21
22
23
24
25
26
27
28
29
30
31
32
33
34
35
36
37
38
39
40
41
42
43
44
45
46
47
48
49
50
51
52
53
54
55
56
57
58
59
60

1
2
3
4
5
6
7
8
9
10
11
12
13
14
15
16
17
18
19
20
21
22
23
24
25
26
27
28
29
30
31
32
33
34
35
36
37
38
39
40
41
42
43
44
45
46
47
48
49
50
51
52
53
54
55
56
57
58
59
60

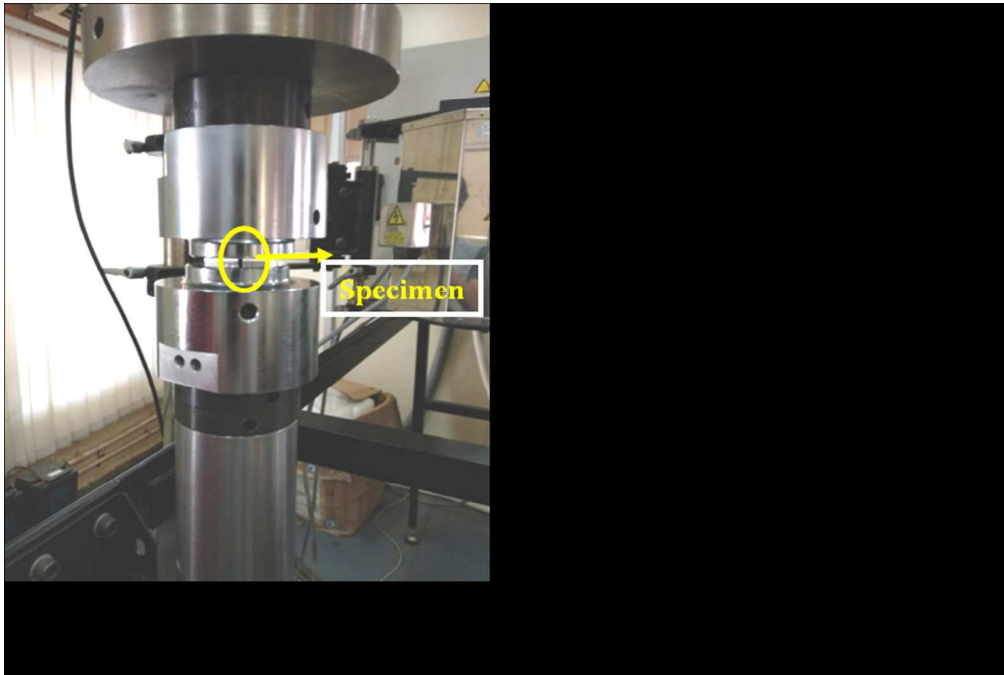


Figure 1. (a) Image of compressive testing machine (b) Schematic diagram of the specimen.

161x108mm (150 x 150 DPI)

View Only

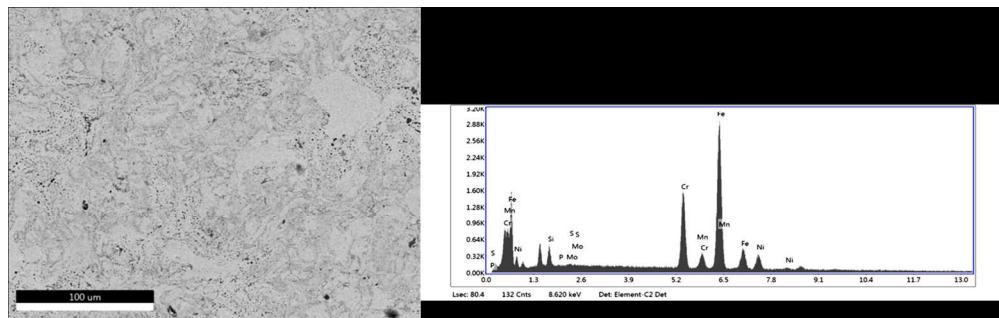


Figure 2. Scanning electron micrograph of unreinforced steel matrix and EDX analysis.

240x75mm (150 x 150 DPI)

Peer Review Only

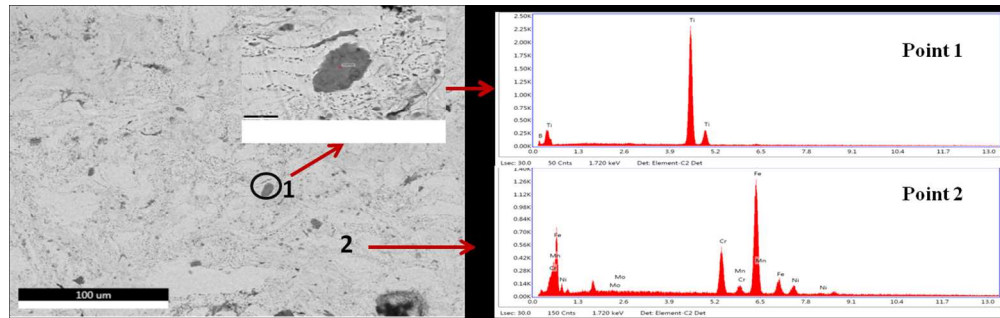


Figure 3. Scanning electron micrograph of composites with 2 vol.% TiB₂ along with EDX of indicated points 1 and point 2.

240x75mm (150 x 150 DPI)

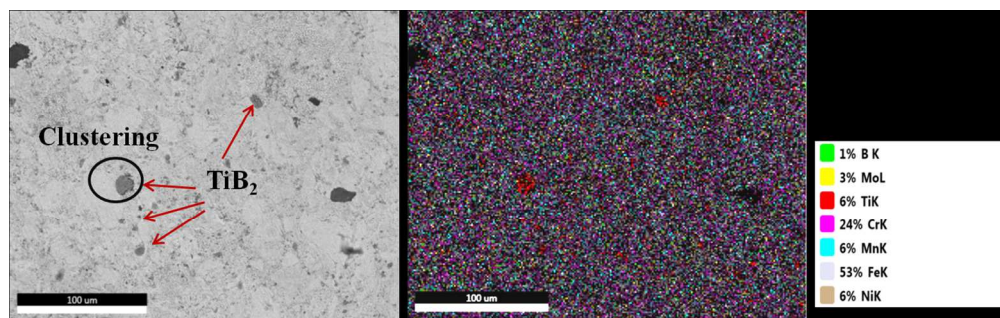


Figure 4. Scanning electron micrograph of composites with 4 vol.% TiB₂ along with EDX mapping.

240x75mm (150 x 150 DPI)

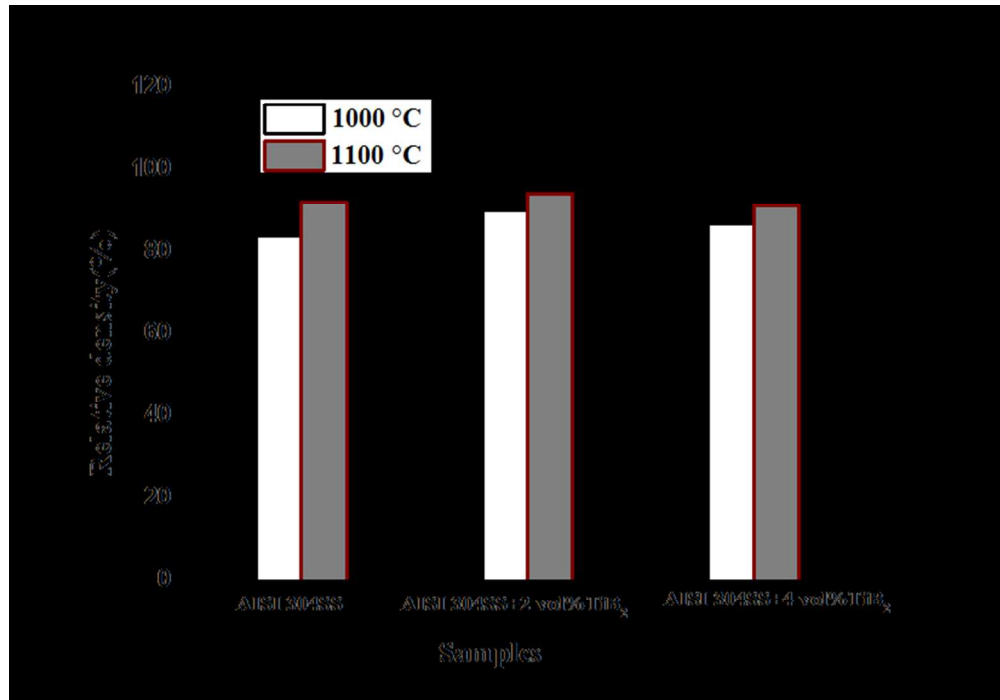


Figure 5. Variation of relative density with the volume percentage of TiB₂.

140x97mm (150 x 150 DPI)

View Only

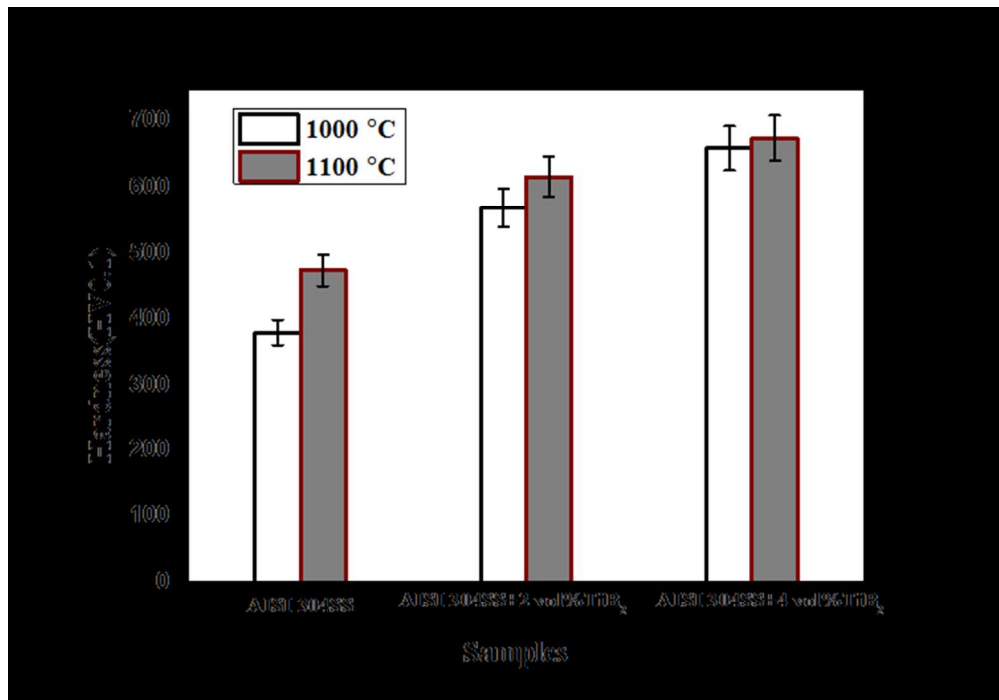


Figure 6. Variation of microhardness with the volume percentage of TiB₂.

128x88mm (150 x 150 DPI)

View Only

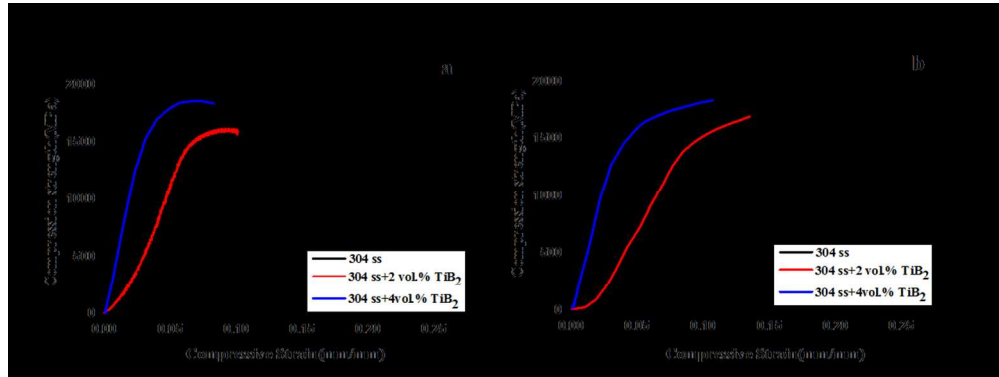


Figure 7. Variation of compression strength of the synthesized composites sintered at (a) 1000 °C and (b) 1100 °C

216x81mm (150 x 150 DPI)

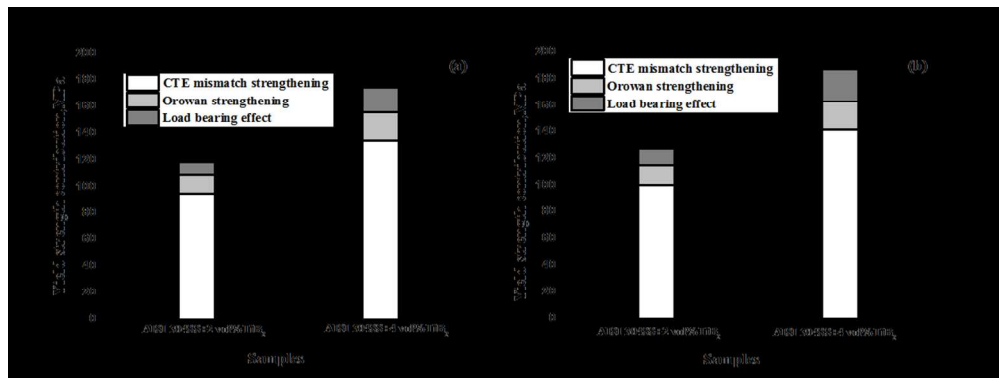


Figure 8. Influence of various strengthening mechanisms in composites sintered at (a) 1000 °C and (b) 1100 °C.

214x80mm (150 x 150 DPI)

Peer Review Only

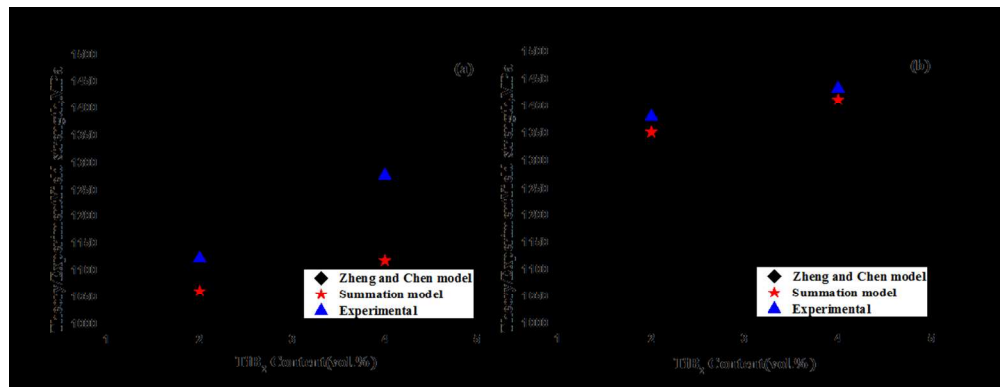


Figure 9. Comparative analysis between numerical models and experimental data sintered at 1000 °C and (b) 1100 °C

212x81mm (150 x 150 DPI)

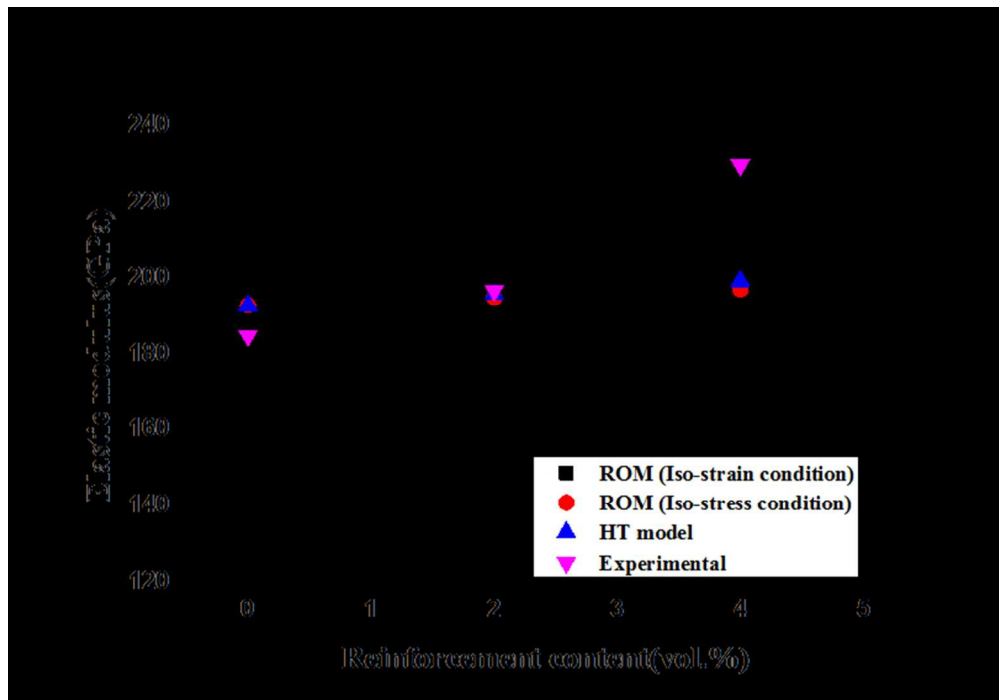


Figure 10. Comparison between experimental and predicted elastic modulus using HT model and ROM.

137x95mm (150 x 150 DPI)

View Only

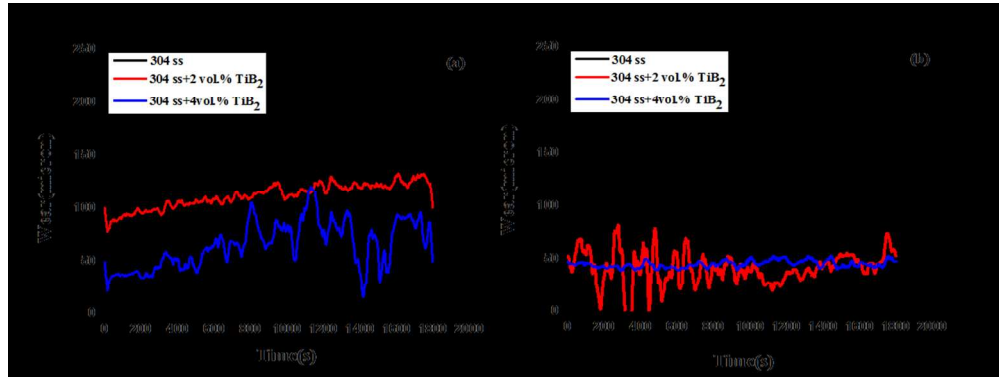


Figure 11. Variation of depth of wear with test time of the synthesized composites sintered at (a) 1000 °C and (b) 1100 °C.

215x80mm (150 x 150 DPI)

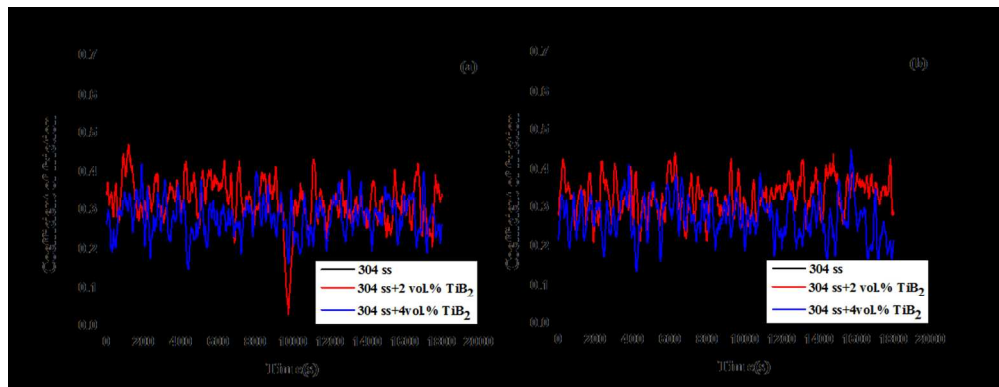


Figure 12. Variation of Coefficient of friction of the synthesized composites with test time sintered at (a) 1000 °C and (b) 1100 °C.

210x81mm (150 x 150 DPI)

1
2
3
4
5
6
7
8
9
10
11
12
13
14
15
16
17
18
19
20
21
22
23
24
25
26
27
28
29
30
31
32
33
34
35
36
37
38
39
40
41
42
43
44
45
46
47
48
49
50
51
52
53
54
55
56
57
58
59
60

Table 1. Composition of AISI 304 Stainless Steel powder (in wt.%)

Grade	C	Mn	Si	P	S	Cr	Mo	Ni	N
AISI304 SS	0.03	2.0	0.75	0.045	0.03	18.0	3.00	10.0	0.10

For Peer Review Only

Table 2.

Material properties and parameters for calculating the improvement of the yield strength (Frost and Ashby 1982).

Properties	Steel matrix	TiB₂ reinforcement
Shear modulus(G_m), GPa	81	191
Burger vector(b), nm	0.258	-
Process temperature, K	1273,1373	1273,1373
Test temperature, K	298	298
Coefficient of thermal expansion (CTE), K ⁻¹	18x10 ⁻⁶	8x10 ⁻⁶
Average particle size (d_p), μm		0.7-0.8